



Published in final edited form as:

J Pharm Sci. 2015 October ; 104(10): 3426–3439. doi:10.1002/jps.24551.

An intravaginal ring for the simultaneous delivery of an HIV-1 maturation inhibitor and reverse transcriptase inhibitor for prophylaxis of HIV transmission

Shweta R. Ugaonkar¹, Justin T. Clark⁴, Lexie B. English¹, Todd J. Johnson¹, Karen W. Buckheit², Robert J. Bahde³, Daniel H. Appella³, Robert W. Buckheit Jr², and Patrick F. Kiser^{1,4,*}

¹University of Utah, Department of Bioengineering, 20 South 2030 East, Salt Lake City, UT, 84112, USA

²ImQuest BioSciences, 7340 Executive Way, Suite R, Frederick, MD, 21704, USA

³Laboratory of Bioorganic Chemistry, NIDDK, NIH, Bethesda, Maryland 20892, USA

⁴Northwestern University, Department of Biomedical Engineering, 2145 Sheridan Rd., Evanston, IL 60208, USA

Abstract

Nucleocapsid 7 (NCp7) inhibitors have been investigated extensively for their role in impeding the function of HIV-1 replication machinery and their ability to directly inactivate the virus. A class of NCp7 zinc finger inhibitors, S-acyl-2-mercaptobenzamide thioesters (SAMTs), was investigated for topical drug delivery. SAMTs are inherently unstable due to their hydrolytically labile thioester bond thus requiring formulation approaches that can lend stability. We describe the delivery of N-[2-(3,4,5-trimethoxybenzoylthio)benzoyl]- β -alanine amide (SAMT-10), as a single agent antiretroviral (ARV) therapeutic and in combination with the HIV-1 reverse transcriptase inhibitor pyrimidinedione IQP-0528, from a hydrophobic polyether urethane (PEU) intravaginal ring (IVR) for a month. The physicochemical stability of the ARV-loaded IVRs was confirmed after 3 months at 40°C/75% relative humidity (RH). *In vitro*, 25 \pm 3 mg/IVR of SAMT-10 and 86 \pm 13 mg/IVR of IQP-0528 were released. No degradation of the hydrolytically labile SAMT-10 was observed within the matrix. The combination of ARVs had synergistic antiviral activity when tested in *in vitro* cell based assays. Toxicological evaluations performed on an organotypic EpiVaginalTM tissue model demonstrated a lack of formulation toxicity. Overall, SAMT-10 and IQP-0528 were formulated in a stable PEU IVR for sustained release. Our findings support the need for further preclinical evaluation.

Keywords

polymeric drug delivery system; stability; epithelial delivery/permeability; HIV/AIDS; mucosal drug delivery; extrusion; biocompatibility; physicochemical properties; preformulation; controlled release

*Corresponding author: Tel: +1- 847-467-5468, patrick.kiser@northwestern.edu.

INTRODUCTION

The use of small molecule antiretroviral agents (ARVs) in pre-exposure prophylaxis (PrEP) of HIV-1 could become an important tool in addressing the global HIV/AIDS public health crisis.¹ Studies show that systemic and topical application of reverse transcriptase (RT) inhibitors for PrEP, such as tenofovir (TFV) or TFV plus emtricitabine², can prevent the sexual transmission of HIV-1. Importantly, it is evident that adherence to the PrEP regimen throughout multiple sexual exposures to HIV-1 is a critical parameter in developing efficacious PrEP agents. Since many women are more prone to acquiring HIV-1 infection, particularly in medium and low income countries, they remain a focus in the global response to the HIV-1 pandemic.^{3,4} As evidenced by the modest efficacy of the TFV gel in the CAPRISA 004 trial⁵ and its lack of significant effect in the VOICE trial⁶, development of long-acting women-controlled drug delivery systems that may increase adherence is imperative. Furthermore, the evolution of resistant HIV-1 strains poses yet another concern in low to middle income countries^{7,8}, and therefore topical PrEP combinations that have a high genetic barrier to resistance need to be evaluated.

The nucleocapsid protein (NCp7) has multiple roles in HIV replication: reverse transcription, integration, Tat transcription, protease production, and incorporation of RNA in budding virions⁹⁻¹³. NCp7 contains two highly conserved zinc finger domains that if mutated, lead to the generation of non-infectious HIV-1 virions. The NCp7 inhibitors have targeted the conserved Zn finger region by stripping the protein of its coordinated Zn²⁺, resulting in the loss of structure and protein function leading to the production of immature virions that are not infectious. Inhibitors from the nitrosobenzamide, disulfide-substituted benzamides, and pyridinioalkanoyl thioester classes were non-specific to HIV-1 NCp7, leading to cytotoxicity^{10,14} and have not been extensively studied for topical application.

The S-acyl-2-mercaptobenzamide thioester (SAMT) chemotype was developed to potentially address the concerns stated above¹³, while congeners have been tested for their ability to block GAG processing¹⁵, prevent infection in murine explants¹⁶, and to study macaque mucosal transmission models¹⁷. SAMTs are also capable of inhibiting cell-to-cell transmission (80 – 100 nM)¹³. However, this class of agents has two notable limitations. First, SAMTs were found not to inhibit initial viral replication in cell-based and tissue explant assays^{13,18}. Second, thioesters are hydrolytically unstable, thereby preventing the chemotype from being delivered via an aqueous gel. Therefore, to target the first round of viral replication and prevent aqueous exposure of SAMT in the formulation, we considered co-delivering a potent pyrimidinedione (PYD) non-nucleoside reverse transcriptase (RT) inhibitor with the SAMT from an elastomeric intravaginal ring. Thus, the RT inhibitor would target the first round of infection and SAMT would prevent dissemination of founder virions if SAMT or the RT inhibitor was unsuccessful at preventing the infection of target cells.

The pyrimidinedione (PYD) derivative 1-cyclopropylmethyl-6-(3,5-dimethyl-benzoyl)-5-isopropyl-1H-pyrimidine-2,4-dione (IQP-0528) is a nanomolar inhibitor of RT and micromolar inhibitor of HIV-1 entry.^{19,20} Recently, characterization and successful delivery of IQP-0528 from a gel formulation^{21,22}, vaginal films²³ and assessment of topical toxicity and vaginal delivery of two PYDs from intravaginal ring formulations²⁴ in pig-tailed

macaques were reported. Although IQP-0528 is a potent non-nucleoside reverse transcriptase inhibitor (NNRTI), resistant strains of HIV-1 for IQP-0528 have been identified (Buckheit *et al.*, unpublished data), whereas resistant strains to SAMTs have not been reported to date. Thus, SAMT/ IQP-0528 combination therapy potentially may be advantageous, because the antiviral properties of each compound can overcome the inadequacies posed by the antiretrovirals (ARVs) alone. The chemical structures and molecular weights (MW) of the SAMT analogues and IQP-0528 are included in Table 1.

Recently, Fetherston et al. reported the delivery of an entry inhibitor and a well-known reverse transcriptase inhibitor from a silicone IVR²⁵. However, there have been no prior systematic formulation development reports for the sustained and long-acting delivery of the SAMT class of compounds. The main objective of this work was to develop a stable delivery system for the hydrolytically labile SAMTs in combination with IQP-0528 in an elastomeric IVR. Herein we report the selection of a lead SAMT analogue, fabrication of the lead SAMT into a stable IVR delivery system in combination with IQP-0528, three-month accelerated stability data, *in vitro* release, *in vitro* efficacy, mechanical analysis, and cytotoxicity testing in a three-dimensional organotypic human EpiVaginal™ tissue model.

MATERIALS AND METHODS

Materials

The SAMT analogues originally were synthesized at the National Institutes of Health (NIH)¹³ (Bethesda, MD) and supplied by ImQuest BioSciences (Frederick, MD) (>95% purity). The supplied SAMT analogues were N-[2-(benzoylthio)benzoyl]-p-alaninamide (SAMT-08), N-[2-(3,4,5-trimethoxybenzoylthio)benzoyl]-β-alanine amide (SAMT-10, D_{90%}: 110 μm), N-[2-(nicotinoylthio)benzoyl]-β-alanine amide (SAMT-19) and N-[2-(acetylthio)benzoyl]-β-alanine amide (SAMT-247). The pyrimidinedione IQP-0528 (D_{90%}: 5 μm) also was supplied by ImQuest BioSciences (Frederick, MD). Tecoflex® EG-85A, a non-swelling polyether urethane (PEU), was purchased from Lubrizol Advanced Materials (Wickliffe, OH). The progestogen 19-norethindrone and HPLC-grade methanol were purchased from Sigma Aldrich (St. Louis, MO). We used 18 MΩ*cm filtered double deionized (DDI) water from a Thermo Scientific Barnstead E-pure system (Ashville, NC). NuvaRing® was purchased from a local pharmacy. A VEC-100 EpiVaginal™ tissue kit was purchased from MatTek Corp. (Ashland, Massachusetts). Solutol® HS 15 was purchased from BASF Corp. (Iselin, NJ). Phosphate-buffered saline (PBS) was purchased from Invitrogen (Carlsbad, CA). All chemicals used were reagent grade and purchased from Sigma Aldrich (99.0% purity).

Methods

Preformulation Testing for the Selection of a lead SAMT Analogue

Thermal Analysis: Thermoanalytical characterization of individual SAMT derivatives were performed using a Mettler Toledo DSC 821e differential scanning calorimeter (DSC). Three to five milligrams of the sample was weighed, sealed in an aluminum pan, and heated at a scanning rate of 10°C/min from 0°C to 300°C. The DSC was calibrated using an indium

standard. The samples were purged using nitrogen at 40 mL/min. The data were analyzed using STAR^e basic software.

Determination of Aqueous Solubility: A saturated solution of each SAMT derivative was prepared in 18 M Ω DDI water and incubated at 37°C while shaking at 250 rpm. Prior to incubation at 37°C, a time zero aliquot was filtered through a 0.2 μ m nylon filter and preserved at –80°C for further analysis. Aliquots of the samples were collected at 24 h and 48 h and treated similarly to the time zero sample. The samples were analyzed by HPLC on a C-18 Zorbax eclipse XDB (5.0 μ m, 4.6 \times 150 mm) reversed-phase column with a gradient of 40% water (mobile phase A) and 60% methanol (mobile phase B) to 100% mobile phase B at a 0.5 mL/min flow rate and a detection wavelength of 285 nm. The HPLC analyses were carried out on an Agilent 1200 series instrument equipped with ChemStation[®] software. This method adequately separated the analyte SAMT peak from the internal standard (norethindrone-19) peak and the degradant peaks (induced at pH 4.0 and 5.0). The limit of quantification (LOQ) was 18.0 pmol.

Chemical Stability of the Analogues at pH 4.0 and 5.0: The SAMT derivatives were tested at physiologically relevant pH (i.e., 4.0 and 5.0). Briefly, 50 μ M stock solutions of the test SAMT derivatives were prepared in 10 mM acetate buffer at pH 4.0 and 5.0 and subjected to 40°C/75% RH incubation. The time zero samples (n=3) were stored at –80°C until further analysis. Aliquots of the samples were obtained at 0 (t=0), 1, 2 and 4 weeks (time 't'), and the drug content was analyzed using HPLC as described earlier. The log concentrations (conc.) plotted vs. time (t) yielded a linear plot. The slope of the line was computed using linear regression. The degradation rate constant (k) was calculated by multiplying the slope by –2.303 per the equation for first order reactions.

Thermal Stability of the SAMT-10: The thermal stability of SAMT-10 (the lead SAMT derivative) was determined by subjecting raw SAMT-10 (powder) to 70°C in a dry atmosphere for a period of three months. Nearly 20 mg of SAMT-10 was placed in amber glass vials (n=3), sealed with a rubber septum and an aluminum cap, and stored at 70°C in a dry atmosphere. The samples were withdrawn at 1 and 3 months and reconstituted in methanol. The recovery at each time point was compared to a control sample that was stored at –20°C during the course of the study. SAMT-10 content was quantified using the HPLC as described previously. The percent recoveries at 1 and 3 months were compared to time zero recovery.

Extrusion Stability of SAMT-10: Upon selection of SAMT-10 as the lead SAMT analogue, the chemical stability of SAMT-10 in the PEU matrix was tested under extrusion conditions. A mixture of 1.0 wt% SAMT-10 in a hydrophobic PEU was extruded at 147°C, and a portion of the extruded rod segment was retained for chemical analysis while the remaining sample was pelletized and re-extruded. This process was repeated for three subsequent extrusion cycles. SAMT-10 was extracted from the rods that were subjected to each extrusion cycle, and the recoveries were compared. ARVs were extracted using a previously developed PEU dissolution-precipitation method.²⁶

Fabrication of Intravaginal Rings (IVR)

SAMT-10 and SAMT-10/IQP-0528 loaded IVRs: The IVRs were fabricated by hot melt extrusion of cryoground PEU mixed with the ARVs using a benchtop twin-screw extruder (ThermoHaake, Waltham, MA) at 147°C, screw speed of 50 rpm and 4.3 mm wide die^{24,26–29}. The target ARV loadings were 1 and 10 wt% SAMT-10 for the single-agent SAMT-10 IVR, 10 wt% for IQP-0528 PEU IVR and 10 wt% each of SAMT-10 and IQP-0528 for the combination SAMT-10/IQP-0528 PEU IVR. To fabricate human-sized IVRs, about 160 mm rod segments (~2.7g) of single agent SAMT-10 (10 wt%) and combination SAMT-10 / IQP-0528 (~ 2.2 g) with a cross-sectional diameter of 4.2 mm were cut, and the ends were joined using a butt-welding kit (Fenner Drives, Manheim PA). The shape of the rings was set in a mold with a 5.5 cm outer diameter at room temperature. The actual loadings of SAMT-10 and IQP-0528 were determined by extraction of ARVs from the polymer matrix as per the method previously published²⁶ and quantified using HPLC as described above. The placebo and the ARV-loaded IVR extrudates were analyzed using a DSC Q-200. Between 5 and 8 mg of each sample was heated from 0°C to 300°C at the rate of 10°C/min. The system was calibrated using indium with a nitrogen purge at 50 mL/min.

Nonoxynol-9 (N-9)-Loaded IVRs: N-9 (5 wt% loading) was added to cryoground PEU and mixed by rolling on a jar mill for 15 min. The N-9 loaded IVR segments were extruded as per the extrusion conditions described above.

Physicochemical Stability of IVRs

Surface Crystallization of the ARVs: Since dissolved molecules often tend to recrystallize on the surface of polymer matrices, which can influence release kinetics³⁰, we monitored the IVRs for surface crystallization at 4°C, RT and 50°C. The IVR segments were observed under a polarized light dissection scope at different time intervals over a period of three months. Cryosectioned films (15 µm) from the IVR matrix also were imaged under an Olympus IX70 polarized light microscope (Center Valley, PA) to observe the surface crystallization.

Accelerated Stability Testing of the Rings: The accelerated chemical stability of the ARVs in the IVR matrix was evaluated over three months using previously described methods.^{26,27} Approximately 50 mg of extruded IVR segments (n=3) were sealed in an aluminum foil pouch and placed in Caron 6030 controlled humidity chambers (Caron, Marietta, OH) at 40°C/75% RH. The stability was evaluated by extracting the ARVs at 1 month and 3 months from the IVR extrudates and comparing the recoveries to the recovery at time zero. The ARVs were extracted using a previously developed PEU dissolution-precipitation method.^{24,26} To determine the extraction efficiency, known amounts of SAMT and IQP-0528 stock solutions were added to placebo samples and 19-norethindrone was added as an internal standard. The chromatographic analysis of IQP-0528 was performed on a C-18 Zorbax eclipse ODS (5.0 µm, 2.5 × 250 mm) reversed-phase column with 45% water (mobile phase A) and 55% acetonitrile (mobile phase B) with a gradient to 80% mobile phase B in 10 min and a 1 mL/min flow rate. The column temperature was 37°C, and the detection wavelengths were 267 nm and 245 nm for SAMT-10 and 19-norethindrone, respectively.

Mechanical Testing—To perform mechanical analysis, the compression/retraction force of the rings was measured using an Instron 3342 (Grove City, PA) mechanical tester and previously described methods.^{26,27} The test was carried out on each sample, and the force required to achieve 25% compression of the initial ring diameter was recorded. The compression profile of the fabricated rings was compared with the compression force of the marketed NuvaRing[®]. The Young's modulus was determined based on the ASTM D412 standard. Specifically, a 25 mm segment was subjected to 10% elongation at a rate of 500 ± 50 mm/min.

In vitro Release Study—The IVR rod segments were prepared for *in vitro* release (n=3) using a previously described method²⁶. Briefly, the rod segments were placed into 25 mM acetate buffer (pH 4.2) containing 2 wt% Solutol[®] HS 15, which provided sink conditions for both IQP-0528 and SAMT-10. For IQP-0528 (single agent) segments, 10 wt% Solutol[®] HS 15 was used to minimize release volumes. The ARV release was quantified using HPLC as described earlier. Upon 30 days release testing, the chemical stability of SAMT-10 in the IVR matrix was confirmed by extraction from both the single agent and combination devices to test for the presence of degradation at pH 4.0 as per the extraction method described earlier^{24,26}. Release data were scaled by length to predict the release from full IVRs.

In vitro release data were further analyzed by fitting to published mathematical models for drug release from IVRs. In cases where the entirety of the ARV loading was solubilized within the polymer matrix, the first 30% of normalized cumulative release (M/M_0) (disregarding day 1 release accounting for potential surface crystallization), were fit to the following equation^{31,32}:

$$\frac{M}{M_0} = \frac{4}{r} \sqrt{\frac{Dt}{\pi}} \quad (1)$$

where, r is the measured cross-sectional radius of the IVR segment and D is the effective Fickian diffusivity in the polymer matrix. D values were calculated for each IVR segment as by re-arranging Eqn. 1 as previously described³². In cases where the majority of the ARV loading was not dissolved in the polymer matrix, normalized residual ARV fractions (M_r/M_0 , equal to $1-M/M_0$) was transformed and fit against linear time according to the following equation, appropriate for predicting drug release from IVRs where drug loading (ω_T) far exceeds the dissolved concentration (ω_s)^{33,34}:

$$\frac{M_r}{M_0} \ln \left(\frac{M_r}{M_0} \right) - \frac{M_r}{M_0} + 1 = \frac{4D\omega_s}{\omega_T r^2} t \quad (2)$$

Since exact values for ω_s were not determined in this study, scaled values of diffusivity ($D^*\omega_s$) were calculated. To estimate the time required to achieve 80% release of SAMT-10 from the SAMT-10/IQP-0528 IVR, we used the calculated value for $D^*\omega_s$, set M_r/M_0 to 0.2, and solved for t .

Safety Evaluation Using a Three Dimensional Organotypic Human Vaginal-Ectocervical Tissue Model—VEC-100 EpiVaginal[™] tissues (partial thickness) (MatTek

Corp.) (n=3) were exposed to placebo and ARV-loaded IVRs (approximately 6 mm in length) in 80 – 85 μL of simulated vaginal fluid [sodium chloride (90.6 mM), sodium lactate (25.5 mM), acetic acid (17.7 mM), pH 4.2]. Untreated tissue samples (naïve, n=3) served as the baseline control, and 5 wt% N-9 loaded segments were used as the cytotoxic control. The samples were incubated at 37°C and 5% CO₂ for seven days. On days 1, 3, 5 and 7 of the study, the basal nutrient media was replaced with fresh pre-warmed nutrient media. Epithelial integrity was monitored on days 1, 3, 5 and 7 using trans epithelial electrical resistance (TEER). On day 7, the tissue viability was determined using an MTT assay, and the samples were fixed in 10% formalin solution for histological analysis. The MTT, TEER and histological evaluations were performed following previously described methods.^{21,22}

Evaluation of Antiviral Activity

Cytopathic Effects (CPE) Inhibition Assay: The CPE assay was performed as previously described³⁵. Briefly, serially diluted compound was added to CEM-SS cells in a 96-well round bottom microtiter plate in triplicate. HIV-1_{IIIIB} at the appropriate pre-determined titer was sequentially added to the microtiter plate and the cultures were incubated at 37°C/5% CO₂ for six days. Following the incubation, the microtiter plates were stained with XTT tetrazolium dye to evaluate the efficacy and toxicity of the test compound(s).

Anti-HIV Assay in Fresh Human Peripheral Blood Mononuclear Cells: PBMC based anti-HIV assays were performed as previously described³⁵. Briefly, PHA-stimulated PBMCs cultured in the presence of IL-2 were suspended at 1×10^6 cells/mL and were added to a 96-well round-bottom plate with serially diluted test materials in triplicate the appropriate pre-titered strain of HIV. The culture was incubated for 7 days at 37°C/5% CO₂. Following the incubation, supernatants were collected for analysis of virus replication by supernatant RT activity and cells analyzed for viability by XTT dye reduction. AZT was used as an internal assay standard.

Inhibition of Cell to Cell Virus Transmission Assay: Uninfected CEM-SS cells were plated in a 96-well flat bottom plate at a density of 1×10^5 cells /well in a total volume of 50 μL . The CEM-SS HIV-1_{IIIIB} chronically infected cells were added at cell densities ranging from 1×10^5 cells per well through to 1×10^0 cells/well in a volume of 50 μL . The test compounds were diluted to 2X the desired high test concentration and were added in triplicate wells in a volume of 100 μL . The plate was incubated at 5% CO₂/37°C for 48 hours. Following the incubation, the number of syncytia per well was counted. Following an additional 24 hour incubation, cell-free supernatant samples from each well of the 96 well plates were analyzed for reverse transcriptase (RT) activity.

Drug Combination Anti-HIV Assays: Using the CPE and PBMC methodologies described above the standard combination anti-HIV assays³⁵ were performed using 5 concentrations of SAMT-10 tested in all possible combinations with 9 concentrations of IQP-0528 in a checkerboard pattern and analyzed for compound interactions at the 95% and 99 and 99.9% confidence intervals using the Prichard and Shipman MacSynergy II software program³⁶. Our extensive experience with the evaluation of combination assay data has resulted in the following interpretations of synergy plot data: $>100 \mu\text{M}^2\%$ is defined as a highly synergistic

interaction; 51 to 99 $\mu\text{M}^2\%$ is defined as synergistic; 0 to 50 $\mu\text{M}^2\%$ and -50 to 0 $\mu\text{M}^2\%$ is defined as additive; -99 to -51 $\mu\text{M}^2\%$ is defined as antagonistic; and <-100 $\mu\text{M}^2\%$ is defined as highly antagonistic.

Statistical analysis—Unless noted, statistical comparisons of data were performed using a two-tailed, heteroscedastic Student's *t*-test, and corresponding *p* values were calculated in Microsoft Excel. Statistical significance was defined as $p < 0.05$.

RESULTS

Selection of the Lead SAMT Analogue

DSC scans of SAMT-08 revealed two melting endotherms at 141°C and 159°C (Figure 1A), which may indicate possible polymorphism. SAMT-19 exhibited a melting endotherm at 161°C followed by an immediate exothermic peak, which indicated thermal degradation (Figure 1B). SAMTs-10 and 247 (Figures 1C and 1D) each had a single melting endotherm at around 183°C and 190°C, respectively, which was higher than the PEU extrusion temperature of 147°C, making them suitable candidates for IVR delivery. IQP-0528 exhibited a melting endotherm at around 216°C (Figure 1E), with no potential degradation or crystal polymorphism and was suitable for delivery with the SAMTs. The physicochemical characteristics of IQP-0528 have been profiled previously²¹. The water solubility of the four SAMT analogues was determined to be 2377.6 ± 27.8 μM for SAMT-08, 332.2 ± 12.7 μM for SAMT-10, 1870.8 ± 199.2 μM for SAMT-19 and 7895.9 ± 338.5 μM for SAMT 247. The recoveries of SAMT analogues in aqueous solution for 1, 2 and 4 weeks and the computed degradation rate constant (*k*) at pH 4.0 and pH 5.0 are given in Tables 2A and 2B, respectively. SAMT-10 exhibited a degradation rate constant greater than SAMT-08 but lower than SAMT-19 and SAMT-247 at both pH 4.0 and 5.0. Overall, the degradation rate constants of different SAMT analogues were comparable under pH 4.0 and 5.0. Furthermore, the dry-state stability of SAMT-10 was not affected by accelerated temperature conditions of 70°C (Figure 2A). The recovery of SAMT-10 from the hydrophobic PEU matrix did not show a statistically significant difference between the first and the third extrusion runs ($p > 0.05$) (Figure 2B), which confirmed the suitability of SAMT-10 for formulation in the PEU matrix.

Fabrication of IVRs

Actual ARV loadings were 0.8 wt% and 7.6 wt% in SAMT-10 single agent IVRs (referred to as “1 wt%” and “8 wt%” throughout), 8.3 wt% SAMT-10 and 9.1 wt% IQP-0528 (also referred to as 8 wt% and 9 wt% respectively throughout) in the combination IVR, and 10.7 wt% in the IQP-0528 single agent IVRs (referred to as “11 wt%” throughout). Lower actual loadings were likely due to process loss and not ARV degradation as confirmed by the stability analyses below. Both IVRs with 8 wt% SAMT-10 were opaque in appearance upon extrusion (Figures 3A and 3B), but 1 wt% SAMT-10 IVR segments were transparent upon extrusion and translucent upon storage (Figure 4A, ii). The SAMT-10 IVR (Figure 3A), SAMT-10/IQP-0528 combination IVR (Figure 3B), and the commercially available NuvaRing[®] (Figure 3C) were comparable in size and diameter. In contrast to the monolithic matrix PEU IVRs presented here, NuvaRing[®] is a solid-core reservoir IVR fabricated from

two grades of poly(ethylene-co-vinyl acetate) (EVA)³⁷. When the extrudates were analyzed using DSC (Figure 3D), the endotherm observed at approximately 70°C in all of the samples could be assigned to the disruption of short-range order domains of the microcrystalline hard segments in the PEUs³⁸. The SAMT-10 melting endotherm was not observed in 1 wt% SAMT-10 IVR segment (Supplementary Figure 1, see Supporting Information). The SAMT-10 melting endotherm in the SAMT-10 IVR (single agent at 8 wt% loading) decreased from 183°C to 166°C (Figure 3D). This decrease in the melting point was attributed to the miscibility of the PEU and the ARV. It is known that the addition of excipients (in this case PEU) to the crystalline samples can serve as an impurity causing broadening and depression of crystal endotherms^{39,40}. Similarly, presence of IQP-0528 (in addition to the PEU) further decreased the MP to 165°C in the SAMT-10/IQP-0528 combination IVR. The endotherm of IQP-0528 at 216°C was not observed in either the IQP-0528 single agent IVR or in combination IVR. This observation indicates that the hydrophobic IQP-0528 was completely miscible or molecularly dispersed within the hydrophobic PEU. As a result the regular crystalline order of IQP-0528 was lost, contributing to the lack of melting endotherm (Figure 3D).

Physicochemical Stability

Surface Crystallization—The macroscopic and cryosectioned images of IVR rod segments after 3 months of storage at 50°C are seen in Figure 4. Figure 4A depicts the macroscopic images of the IVR rod segments of the placebo (Figure 4A–i), the single agent SAMT-10 (1 and 8 wt%, Figures 4A–ii and -iii respectively), and the combination SAMT-10/IQP-0528 PEU IVR matrix samples (Figure 4A–iv). Surface crystal formation was not observed at the macroscopic scale, except for in the 1 wt% SAMT-10 IVR (4A–ii). To further characterize the surface crystallization, 15 µm thick cryosections were microscopically observed (Figure 4B). Figure 4B shows images of the cryosections of the corresponding IVR segments from Figure 4A. In Figure 4B, the transparent core of the placebo PEU IVR (Figure 4B–i) is obvious. Microscopic observation of the 1% SAMT-10 IVR (Figure 4B–ii) confirmed surface crystallization, but did not reveal any core crystallization, thus indicating that the SAMT-10 loaded had been solubilized by the PEU matrix, likely in a supersaturated state. The 8 wt% SAMT-10 IVR matrix and the SAMT-10/IQP-0528 IVR combination matrix did not show preferential surface crystal formation, even after 3 months at 50°C. There was an absence of birefringence on the edge (surface), which is a characteristic of surface crystallization²⁷. The core of the ARV-loaded matrices showed uniform particulate distribution.

Chemical Stability of the SAMT Derivatives—Normalized recovery of SAMT-10 (Figure 4C) and IQP-0528 (Figure 4D) at time zero and three months under accelerated conditions (40°C/75% RH) from both 8% SAMT-10 IVR matrices (single agent and combination) were comparable ($p > 0.05$, two-tailed, Student's *t* test). The recoveries of spiked SAMT-10 and IQP-0528 were 100.3 ± 0.95 and $99.2 \pm 0.12\%$, respectively. The stability of pyrimidinedione derivatives including IQP-0528 in PEU matrix has been reported previously²⁴.

Mechanical Testing

The force required to compress the IVRs to 25% of their original outer diameters were 0.91 N for the 8 wt% loaded SAMT-10 IVR and 0.81 N for the combination SAMT-10/IQP-0528 IVR. For comparison, the compression force of NuvaRing® was measured at 1.45 N. As the IQP-0528 loading in the IVRs increased, the compression force reduced, which was likely due to the plasticization effect of the highly soluble IQP-0528. The resulting values for Young's modulus were 20.2 ± 1.2 MPa for the SAMT-10 IVR matrix, 14.33 ± 0.8 MPa for the combo IVR matrix, which are comparable to literature reports of an effective Young's Modulus for NuvaRing® (approximately 18 MPa⁴¹).

In vitro Release

The *in vitro* release of SAMT-10 and IQP-0528 from single agent and combination PEU matrices under sink conditions is presented in Figure 5. Cumulative release (CR) of SAMT-10 and IQP-0528 is shown in Figures 5A and 5C respectively while daily release (DR) of SAMT-10 and IQP-0528 is shown in Figures 5B and 5D respectively. As seen from the release profiles, $10.6 \pm 0.8\%$ (25 ± 3 mg/IVR) of SAMT-10 and $27.3 \pm 4.1\%$ (86 ± 13 mg/IVR) of IQP-0528 were released from the combination IVR at the end of 30 days, which implies that the SAMT-10/IQP-0528 IVR formulation was suitable for long-acting delivery (N=3, mean \pm SD). By mass, the release of IQP-0528 from the combination IVR was nearly 3.5 times greater than the release of SAMT-10 from the same device. The cumulative percentage of SAMT-10 released from the combination formulation was significantly higher ($p = 0.04$) than the amount of SAMT-10 released from the IVR that only contained SAMT-10 ($10.6 \pm 0.8\%$ vs. $8.8 \pm 0.3\%$, N=3, mean \pm SD), which indicated that the presence of IQP-0528 resulted in increased flux of SAMT-10 from the IVR matrix (Figure 5A). By extrapolation using Eqn. 3, we estimate that it would take 2461 days (approximately 6.7 years) to release 80% of the SAMT-10 loaded into the SAMT-10/IQP-0528 IVR. Following release testing, SAMT-10 was re-extracted from both of the formulations. No degradants characteristic of pH 4.0 degradation were observed. This confirmed that the SAMT-10 had not undergone chemical modification within the matrix during 30 day release testing. SAMT-10 release from the 8% (single agent) and 1% IVR formulation is compared in figures 5E (CR) and 5F (DR). SAMT-10 release was not loading-dependent between the two loadings tested. The 8-fold increase in SAMT-10 loading only resulted in a 52% increase in 30-day cumulative release ($22.9 \pm 1.1\%$ vs. 15.1 ± 1.9 , N=3, mean \pm SD). These data agree with the DSC analysis and macro and microscopic evaluation (Figures 3 and 4), confirming that the 8 wt% SAMT-10 was not completely solubilized.

Release data were well fit by the models applied. SAMT-10 (8 wt%) release data from the combination SAMT-10/IQP-0528 IVR and SAMT-10 only IVR fit well when a linear regression was applied to plots of transformed CR against time (Eqn. 2, $R^2 > 0.992$, individual samples from both datasets) as shown in Figure 5G. The scaled SAMT-10 diffusivity ($D^*\omega_s$) in the polymer matrix, as calculated per Equation 2 was 31% higher in combination with IQP-0528 ($1.9 \pm 0.3 \times 10^{-12}$ cm²/s vs. $1.3 \pm 0.1 \times 10^{-12}$ cm²/s, N=3, mean \pm SD), indicating either a higher SAMT-10 diffusivity or increased solubilization due to the presence of dissolved IQP-0528. Although the higher flux of SAMT-10 was statistically significant (above), the difference in diffusivity readings was slightly above the

threshold for significance ($p = 0.06$). SAMT-10 release from 1% SAMT-10 IVR and IQP-0528 release from both the combination and single agent IVRs were well fit by linear regressions against the square-root-of-time, as shown in Figure 5H (Eqn. 2, $R^2 > 0.999$, $R^2 > 0.998$ and $R^2 > 0.982$ for individual samples, respectively). SAMT-10 release from the 1 wt % IVR was only fitted to day 6 (30% mean CR), because Eqn. 2 loses accuracy beyond 30% CR³¹. Nonlinearity in cumulative release against the square-root-of-time were observed later in the 30 day curve as expected³¹. SAMT-10 exhibited a diffusivity of $2.1 \pm 0.3 \times 10^{-9}$ cm²/s (N=3, mean \pm SD) in the 1% SAMT-10 IVR. Comparison of SAMT-10 diffusivity in the 1% IVR to $D^* \omega_s$ calculated for the 8% single agent IVR, assuming SAMT-10 diffusivity in outside the diffusion front is not altered following the dissolution of SAMT-10 particles, suggests that 0.07% w/w SAMT-10 was dissolved in the 8 wt% SAMT-10 IVR formulation. This value is roughly an order of magnitude less than that dissolved in the “1%” IVR (actual loading approximately 0.8% w/w). IQP-0528 diffusivity was 27% lower in the presence of 8% SAMT-10 ($3.9 \pm 0.4 \times 10^{-10}$ cm²/s, single agent vs. $2.8 \pm 0.8 \times 10^{-10}$ cm²/s, combination, N=3, mean \pm SD), although the decrease was not statistically significant ($p = 0.13$).

Safety Evaluation using an Organotypic Human 3D Vaginal Tissue Model

Organotypic Tissue Viability—As expected, tissue viability following exposure to the N-9 treated IVR was $4.1 \pm 0.7\%$, which was significantly lower ($p < 0.001$) than for tissues exposed naïve and ARV-loaded IVRs (Figure 6A). Tissue viability following exposure to the SAMT-10 loaded IVR and the combination SAMT-10/IQP-0528 IVR were determined to be $95.5 \pm 5.1\%$ and $98.2 \pm 1.7\%$, respectively. These differences were not statistically significant compared to naïve tissue (Figure 6A). The data indicates that even after dosing for 7 days in an *in vitro* organotypic tissue model, the samples (ARV loaded IVR segments) were not toxic.

TEER Evaluation—The structural integrity of the tissues was routinely monitored throughout the seven day study period. In accordance with the tissue viability data, N-9 treated tissues showed a significant drop in the TEER values on day 1 and remained significantly low on days 3, 5 and 7 ($p < 0.001$) (Figure 6B). The recorded TEER values in the N-9 treated cells implicate a loss of structural integrity because the TEER is a measure of barrier resistance offered by the tissue cell layers. However, the measured TEER values in the tissues treated with IVRs did not exhibit a decrease. There was a transient increase in TEER values of the tissues treated with IVRs on days 3, 5 and 7.

Histological Analysis—The surface epithelial layers and the basal membrane of the naïve tissues were clearly differentiated (Figure 6C). N-9 treated tissues showed a complete loss of the surface epithelium, which was consistent with the cell viability and TEER observations. In the SAMT-10 IVR treated tissue and the SAMT-10/IQP-0528 combination IVR treated tissue, the morphological responses were similar to the responses observed in the naïve tissue. Specifically, epithelial integrity was intact, even after a seven-day dosing period. The histology further supported the cell viability and TEER measurements, further confirming the safety of the test formulations in the VEC-100 EpiVaginal™ tissues.

In Vitro Efficacy Evaluations

Efficacy of IQP-0528 and SAMT-10—IQP-0528 and SAMT-10 were evaluated in three *in vitro* assays to determine anti-HIV efficacy (Table 3). In CEM-SS cells tested against the laboratory-derived strain HIV-1_{IIIIB}, IQP-0528 was active at a 95% inhibitory concentration (EC₉₅) of 0.008 μM and SAMT-10 was active at 2.9 μM . In human PBMCs tested against a clinical subtype C CCR5-tropic strain of HIV-1, the EC₉₅ of IQP-0528 was 0.019 μM and the activity of SAMT-10 9.6 μM in one of three experiments. In the other two repeat experiments the exact EC₉₅ could not be determined, but a lower bound of 10 μM was estimated. In a cell-to-cell transmission assay where uninfected CEM-SS cells were incubated with chronically infected HIV-1_{RF} CEM-SS cells (an efficacy assay that is typically used for agents which cause virus inactivation) the EC₉₅ was 0.085 μM for IQP-0528 and 9.1 μM for SAMT-10. EC₅₀ values were also calculated for each assay, and are listed in Table 3. Given the antiviral activity of these APIs and their different mechanisms of action the compounds were further evaluated in *in vitro* cell-based combination assays to determine how they would interact to inhibit virus when used as a component of a combination topical PrEP agent product.

Efficacy of IQP-0528 in Combination with SAMT-10—IQP-0528 and SAMT-10 were evaluated for activity and cellular toxicity in combination assays performed in CEM-SS cells with the laboratory-derived HIV-1_{IIIIB} and in human PBMCs with the clinical strain HIV-1_{ZA/97/009} (Table 4). The combination product interaction was determined utilizing the Prichard and Shipman MacSynergy II methodology³⁶. In these combination antiviral assays the activity of the two compounds together was compared to the activity of the two compounds when used alone to derive their synergy volumes at 95, 99 and 99.9% confidence intervals. In this assay the concentrations utilized for each compound at the EC₅₀ and at serial 2-fold dilutions below the EC₅₀ were evaluated. Based on our extensive history of use of the MacSynergy II program and evaluation of hundreds of combination assays, $>100 \mu\text{M}^2\%$ is defined as a highly synergistic interaction; 51 to 99 $\mu\text{M}^2\%$ is defined as synergistic; 0 to 50 $\mu\text{M}^2\%$ and -50 to 0 $\mu\text{M}^2\%$ is defined as additive; -99 to $-51 \mu\text{M}^2\%$ is defined as antagonistic; and $<-100 \mu\text{M}^2\%$ is defined as highly antagonistic. In CEM-SS cells tested against HIV-1_{IIIIB} the combination of IQP-0528 and SAMT-10 was determined to be highly synergistic and in PBMCs tested against HIV-1_{ZA/97/009} the combination was additive. Both of these results would indicate that these two compounds would yield a favorable topical PrEP agent combination product since no evidence of antagonism or combination toxicity was observed (data not shown).

DISCUSSION

The present work demonstrates the delivery of two structurally and mechanistically divergent ARVs, the NCp7 inhibitor SAMT-10 and the hydrophobic entry inhibitor-NNRTI IQP-0528. The ARVs were formulated in a matrix intravaginal ring fabricated from a biomedical grade PEU^{26–29}. This hydrophobic polymer was capable of solubilizing both ARVs and protecting the SAMT from hydrolysis. Characterization of the system included determination of the thermoanalytical profiles, aqueous solubility, and degradation rates at physiologically relevant pH of 4.0 and 5.0, monitoring the release of the lead SAMT-10

from single agent and combination (with IQP-0528) IVR segments for 30 days, physicochemical stability, and assessing safety and efficacy of the ARV loaded IVR segments.

SAMT-10 was selected from the library of SAMT compounds since it exhibited a single sharp endotherm well above the processing temperature (no thermal degradation under the processing conditions) with greater hydrophobicity (relative to other SAMT analogues) and a relatively slow rate of degradation under physiological pH conditions. In addition, while SAMT-10 does not exhibit particularly good solubility in the hydrophobic polyether urethane elastomer, SAMT-10 can be dissolved in the matrix following extrusion to allow for its release from the matrix by diffusion⁴². To confirm extrusion stability, SAMT-10 recovered from PEU exposed to three repeated extrusion cycles indicated no significant loss between the extrusion cycles. In addition, the mixture is likely to undergo only one round of extrusion during the actual manufacturing process, further supporting the feasibility of extruding SAMT-10 in a hydrophobic PEU matrix. After three months of storage under accelerated conditions (40°C/75% RH), the fabricated IVRs showed chemical stability for the ARVs in the PEU matrix. Physical stability also was observed (i.e., there was no surface crystal growth during the three months of storage at 50°C).

The *in vitro* release of IQP-0528 was approximately 3.5 times greater than SAMT-10 by mass, while both the ARVs exhibited matrix kinetics. A higher initial dose due to matrix kinetics is potentially advantageous, as it could act as a loading dose after the ring is inserted. The increased flux for IQP-0528 was expected because IQP-0528 has better solubility in the hydrophobic PEU matrix. Mathematical modeling estimated that 80% CR of SAMT-10 from the SAMT-10/IQP-0528 IVR would take nearly 7 years, indicating that, considering the nonlinear loading dependence of SAMT-10, it may be possible to reduce drug loading and decrease excess, depending on the eventual drug release rates targeted.

Complete or near-complete solubilization of 9 to 11 wt% IQP-0528 in the PEU matrix of the combination IVR is supported by DSC analysis of the ARV-loaded extrudates where the melting endotherm of IQP-0528 was not observed in the PEU matrix, whereas the relatively less hydrophobic SAMT-10 remained largely dispersed within the matrix and elicited a melting endotherm at 165°C. The decrease in the melting point of the SAMT-10 from 183°C to 165°C was due to its partial dissolution in the polymer. Furthermore, the solubilities of the ARVs were assessed qualitatively by evaluating the appearance of the IVR. The 11 wt% loaded IQP-0528 PEU IVR appeared transparent, whereas the 8 wt% SAMT-10 IVR is opaque white upon extrusion. The core of the 1 wt% loaded SAMT-10 PEU IVR was translucent, indicating that the entirety of the 0.8 wt% was solubilized by the PEU. However, the surface crystallization present indicates a supersaturated state, and that the equilibrium solubility is lower than 0.8 wt% (exact value not determined). By applying two differing mathematical models to SAMT-10 release from the 1 wt% SAMT-10 IVR (core ARV completely solubilized) and the 8 wt% SAMT-10 (single agent) formulations (ARV mostly dispersed), we calculated that the scaled diffusivity ($D^*\omega_s$) was over an order of magnitude less than expected (assuming that ω_s would be at least 0.8%). This suggests that either, 1) transport through the PEU matrix is hindered following depletion of undissolved SAMT-10, or 2) ω_s is much lower than 0.8 wt% (known to be above saturation based on surface

crystallization). In a previous elastomeric IVR formulation, lower degrees of supersaturation were observed with increasing ARV loading³⁷, meaning that, upon fabrication, ω_s may decrease with increasing ω_T . It is likely that both changes in the matrix and a decrease in solubilization contributed to the lower than expected release. We conclude that IQP-0528 was completely (or near-completely) dissolved in the combination IVR, and that SAMT-10 was mostly undissolved, ultimately resulting in a higher flux of IQP-0528 than SAMT-10. Interestingly, the presence of 9 wt% dissolved IQP-0528 in the formulation contributed to higher diffusivities (and corresponding fluxes) of SAMT-10. Analogous to the previous explanation, this could be due to an increase in SAMT-10 solubilization in the presence of IQP-0528, or due to multi-component effects, whereby IQP-0528 flux increases the effective diffusivity of SAMT-10 once dissolved in the formulation. In contrast, IQP-0528 diffusivity was reduced in the combination IVR formulation, indicating that the presence of undissolved SAMT-10 crystals (or pores resulting from SAMT-10 dissolution into the matrix) hinder IQP-0528 transport. IQP-0528 %CR from the single agent (11 wt%) IVR was much lower than our previously published data, which tested a much lower loading (0.5 wt %) in the same polymer, which may indicate concentration dependent diffusivity at such high levels of dissolved IQP-0528.

Upon extrusion, IQP-0528 was miscible in the PEU matrix at the concentrations tested and remained in the dissolved state in the PEU matrix throughout the stability testing period. PEU-soluble SAMT-10 was completely solubilized at 1% w/w but formed a crystalline dispersion at 8% w/w upon extrusion, which did not undergo any further significant crystalline changes during the three months of storage at accelerated conditions.

Compression testing indicated that the measured compression force ($F_{25\%}$) for the combination IVR was lower than the SAMT-10 IVR, and this decrease was attributed to the solubilized IQP-0528, which may act as a plasticizer of the PEU⁴³. Nevertheless, the mechanical properties of the SAMT-10 IVR, the combination SAMT-10/IQP-0528 IVR, and NuvaRing[®] were comparable. NuvaRing[®] has shown a high acceptability (96 – 97%) among women when tested for ease of use, discretion, and partner acceptability⁴⁴. Therefore, the results from the mechanical testing confirmed that the mechanical characteristics of the fabricated IVRs will likely be suitable for intravaginal use.

Another significant aspect of this IVR is that the PEU protected SAMT-10 from degradation in the aqueous release media. A more hydrophilic polymer increased the release rate of SAMT-10 (data not shown), however, the SAMT-10 thioester was more susceptible to aqueous degradation in these more polar matrices because of the activity of water. SAMT-10 hydrolysis occurs when the thiol group is cleaved to form 3-(3-oxobenzol[d]isothiazol-2(3H)-yl) propanamide and 3,4,5-trimethoxybenzoic acid. An analysis of SAMT-10 in the IVR matrix by HPLC after 30 days of release did not indicate the presence of degradants seen when SAMT-10 is solubilized in pH 4 media.

To confirm clinical viability, topical PrEP agents must be evaluated for safety and tolerability³. In the present study we studied the toxicity of the ARV-loaded extrudates in an organotypic 3D EpiVaginal[™] tissue model under repeated dosing for seven days. N-9⁴⁵ and cellulose sulfate trials⁴⁶ have drawn attention to the safety evaluation of topical PrEP agents,

because the use of surfactant-based vaginal products have demonstrated an increase the risk of HIV-1 infection^{47,48}. The EpiVaginal™ tissue model used in the present study is reproducible and bears structural and physiological resemblance to the human vaginal epithelium and was specifically designed to study the effects of topical PrEP agents on the vaginal epithelium⁴⁹. Also, the model allows testing of continuous daily dose application for multiple days. In the present study, cell death and lower TEER values were seen for the N-9 toxic control, whereas the single agent SAMT-10 IVR and the SAMT-10/IQP-0528 combination IVR displayed cell viability and TEER values that were comparable to the naïve tissues. The transient increase in the TEER values of the tissues treated with IVRs on days 3, 5 and 7 may be attributed to the constant cell growth seen in culture media as this increase was also observed for the placebo tissues. Histological evaluations suggested complete disruption of the epithelium in the N-9 treated tissues and conserved structural integrity of the epithelium in the ARV-loaded IVRs.

The antiviral activities of the single agent SAMT-10 IVR and the SAMT-10/IQP-0528 combination IVR were evaluated in HIV-1 inhibition cell based and in human ectocervical explants assays challenged with HIV-1. The only way to evaluate if a drug will prevent mucosal transmission of HIV is to evaluate it in an animal model where careful PK and subsequent challenge studies are coupled^{50,51}. During the development of drug delivery systems for HIV prevention target tissue or biofluid concentrations are often set at four times the EC₉₅. This value is approximately 40 µM for SAMT-10 based highest *in vitro* measurement of the EC₉₅. Assuming sink conditions exist for SAMT-10, diluting the minimum release rate observed from the dual agent IVR (440 µg per day), into the maximum daily vaginal fluid volume expected (~10 mL), yields an estimate of 100 µM SAMT-10, demonstrating that the present system has potential to provide SAMT-10 concentrations that could significantly suppress viral replication in the vaginal mucosa. Synergistic to additive effect of the combination ARVs was observed *in vitro*. The overall activity of the SAMT-10/IQP-0528 combination IVR was observed to be greater than the SAMT-10 alone IVR in CPE assay. Moreover, we also have shown that human ectocervical explants when challenged with HIV-1 were completely protected by SAMT-10 IVR and SAMT-10/IQP-0528 combination IVR with greater than 1 order of magnitude decrease in HIV-1 p24 and lack of HIV-1 infected cells as measured by immunohistochemistry (unpublished observations).

Adherence and cost effectiveness have emerged as critical factors that shape the overall user acceptability of medication in developing countries. An ARV vaginal gel application is estimated to cost nearly 5 dollars per month⁵². Considering that an IVR will be used once per month, we estimate that the IVRs can be provided at costs competitive to episodic dosage forms such as gels. Thus, a long-acting combination IVR topical PrEP agent would likely address adherence and cost issues.

The present study demonstrated successful and sustained delivery of an NCP7 inhibitor (SAMT-10) in combination with a dual-acting entry inhibitor NNRTI, IQP-0528, from a physicochemically stable IVR formulation. Successful development initiatives included the selection of a lead SAMT analogue and its fabrication into a solid IVR dose form in combination with IQP-0528. We also established the physicochemical stability under

accelerated conditions and the *in vitro* safety and efficacy. These results support the use of intravaginal delivery of a SAMT-10/IQP-0528 combination and encourages further preclinical investigation.

Supplementary Material

Refer to Web version on PubMed Central for supplementary material.

Acknowledgments

This work was supported by NIH grant # 5U19AI077289.

ABBREVIATIONS

ARV	antiretroviral
CR	cumulative (ARV) release
DR	daily (ARV) release
IVR	intravaginal ring
PEU	poly(ether urethane)
PrEP	pre-exposure prophylaxis
PYD	pyrimidinedione
RT	(HIV-1) reverse transcriptase
SAMT	S-acyl-2-mercaptobenzamide thioester

References

1. Person AK, Hicks CB. Pre-exposure prophylaxis--one more tool for HIV prevention. *Curr HIV Res.* 2012; 10(2):117–122. [PubMed: 22329517]
2. Celum C, Baeten JM. Tenofovir-based pre-exposure prophylaxis for HIV prevention: evolving evidence. *Curr Opin Infect Dis.* 2012; 25(1):51–57. [PubMed: 22156901]
3. U.S. Food and Drug Administration. Center for Drug Evaluation and Research. Guidance for Industry. Vaginal microbicides: Development for the prevention of HIV infection. 2014. <http://www.fda.gov/downloads/drugs/guidancecomplianceregulatoryinformation/guidances/ucm328842.pdf>
4. UNAIDS. UNAIDS report on the global aids pandemic 2010. 2010. ed
5. Valley-Omar Z, Sibeko S, Anderson J, Goodier S, Werner L, Arney L, Naranbhai V, Treurnicht F, Abrahams MR, Bandawe G, Swanstrom R, Karim QA, Karim SS, Williamson C. CAPRISA 004 Tenofovir Microbicide Trial: No Impact of Tenofovir Gel on the HIV Transmission Bottleneck. *J Infect Dis.* 2012
6. McEnery R. Oral tenofovir arm of VOICE trial discontinued early. *IAVI Rep.* 2011; 15(5):21.
7. Shao Y, Williamson C. The HIV-1 Epidemic: Low- to Middle-Income Countries. *Cold Spring Harb Perspect Med.* 2012; 2(3):a007187. [PubMed: 22393534]
8. Grant RM, Hamer D, Hope T, Johnston R, Lange J, Lederman MM, Lieberman J, Miller CJ, Moore JP, Mosier DE, Richman DD, Schooley RT, Springer MS, Veazey RS, Wainberg MA. Whither or wither microbicides? *Science.* 2008; 321(5888):532–534. [PubMed: 18653884]

9. de Rocquigny H, Shvadchak V, Avilov S, Dong CZ, Dietrich U, Darlix JL, Mely Y. Targeting the viral nucleocapsid protein in anti-HIV-1 therapy. *Mini Rev Med Chem*. 2008; 8(1):24–35. [PubMed: 18220982]
10. Jim A, Turpin MLS, Miller Jenkins Lisa M, Inman John K, Appella Ettore. Topical Microbicides: A promising approach for controlling the AIDS pandemic via retroviral Zinc finger inhibitors. *Advances in Pharmacology*. 2008; 56:229–256. [PubMed: 18086414]
11. Musah RA. The HIV-1 nucleocapsid zinc finger protein as a target of antiretroviral therapy. *Curr Top Med Chem*. 2004; 4(15):1605–1622. [PubMed: 15579099]
12. Rice WG, Supko JG, Malspeis L, Buckheit RW Jr, Clanton D, Bu M, Graham L, Schaeffer CA, Turpin JA, Domagala J, Gogliotti R, Bader JP, Halliday SM, Coren L, Sowder RC 2nd, Arthur LO, Henderson LE. Inhibitors of HIV nucleocapsid protein zinc fingers as candidates for the treatment of AIDS. *Science*. 1995; 270(5239):1194–1197. [PubMed: 7502043]
13. Srivastava P, Schito M, Fattah RJ, Hara T, Hartman T, Buckheit RW Jr, Turpin JA, Inman JK, Appella E. Optimization of unique, uncharged thioesters as inhibitors of HIV replication. *Bioorg Med Chem*. 2004; 12(24):6437–6450. [PubMed: 15556761]
14. Valerie Goldschmidt LMMJ, Hugues de Rocquigny, Jean-Luc Darlix, Yves Mely. The nucleocapsid protein of HIV-1 as a promising therapeutic target for antiviral drugs. *HIV Therapy*. 2010; 4(2):179.
15. Miller Jenkins LM, Ott DE, Hayashi R, Coren LV, Wang D, Xu Q, Schito ML, Inman JK, Appella DH, Appella E. Small-molecule inactivation of HIV-1 NCp7 by repetitive intracellular acyl transfer. *Nat Chem Biol*. 2010; 6(12):887–889. [PubMed: 20953192]
16. Schito ML, Goel A, Song Y, Inman JK, Fattah RJ, Rice WG, Turpin JA, Sher A, Appella E. In vivo antiviral activity of novel human immunodeficiency virus type 1 nucleocapsid p7 zinc finger inhibitors in a transgenic murine model. *AIDS Res Hum Retroviruses*. 2003; 19(2):91–101. [PubMed: 12639244]
17. Schito ML, Soloff AC, Slovit D, Trichel A, Inman JK, Appella E, Turpin JA, Barratt-Boyes SM. Preclinical evaluation of a zinc finger inhibitor targeting lentivirus nucleocapsid protein in SIV-infected monkeys. *Curr HIV Res*. 2006; 4(3):379–386. [PubMed: 16842089]
18. Wallace GS, Cheng-Mayer C, Schito ML, Fletcher P, Miller Jenkins LM, Hayashi R, Neurath AR, Appella E, Shattock RJ. Human immunodeficiency virus type 1 nucleocapsid inhibitors impede trans infection in cellular and explant models and protect nonhuman primates from infection. *J Virol*. 2009; 83(18):9175–9182. [PubMed: 19587055]
19. Buckheit RW Jr, Hartman TL, Watson KM, Kwon HS, Lee SH, Lee JW, Kang DW, Chung SG, Cho EH. The structure-activity relationships of 2,4(1H,3H)-pyrimidinedione derivatives as potent HIV type 1 and type 2 inhibitors. *Antivir Chem Chemother*. 2007; 18(5):259–275. [PubMed: 18046959]
20. Buckheit RW Jr, Hartman TL, Watson KM, Chung SG, Cho EH. Comparative evaluation of the inhibitory activities of a series of pyrimidinedione congeners that inhibit human immunodeficiency virus types 1 and 2. *Antimicrob Agents Chemother*. 2008; 52(1):225–236. [PubMed: 17967909]
21. Mahalingam A, Simmons AP, Ugaonkar SR, Watson KM, Dezzutti CS, Rohan LC, Buckheit RW Jr, Kiser PF. Vaginal Microbicide Gel for Delivery of IQP-0528, a Pyrimidinedione Analog with a Dual Mechanism of Action against HIV-1. *Antimicrob Agents Chemother*. 2011; 55(4):1650–1660. [PubMed: 21245437]
22. Ham AS, Ugaonkar SR, Shi L, Buckheit KW, Lakouagna H, Nagaraja U, Gwozdz G, Goldman L, Kiser PF, Buckheit RW Jr. Development of a combination microbicide gel formulation containing IQP-0528 and tenofovir for the prevention of HIV infection. *J Pharm Sci*. 2012; 101(4):1423–1435. [PubMed: 22227864]
23. Ham AS, Rohan LC, Boczar A, Yang L, WB K, Buckheit RW Jr. Vaginal film drug delivery of the pyrimidinedione IQP-0528 for the prevention of HIV infection. *Pharm Res*. 2012; 29(7):1897–1907. [PubMed: 22392331]
24. Johnson TJ, Srinivasan P, Albright TH, Watson-Buckheit K, Rabe L, Martin A, Pau CP, Hendry RM, Otten R, McNicholl J, Buckheit R Jr, Smith J, Kiser PF. Safe and sustained vaginal delivery of pyrimidinedione HIV-1 inhibitors from polyurethane intravaginal rings. *Antimicrob Agents Chemother*. 2012; 56(3):1291–1299. [PubMed: 22155820]

25. Fetherston SM, Boyd P, McCoy CF, McBride MC, Edwards KL, Ampofo S, Malcolm RK. A silicone elastomer vaginal ring for HIV prevention containing two microbicides with different mechanisms of action. *Eur J Pharm Sci.* 2013; 48(3):406–415. [PubMed: 23266465]
26. Johnson TJ, Gupta KM, Fabian J, Albright TH, Kiser PF. Segmented polyurethane intravaginal rings for the sustained combined delivery of antiretroviral agents dapivirine and tenofovir. *Eur J Pharm Sci.* 2010; 39(4):203–212. [PubMed: 19958831]
27. Clark MR, Johnson TJ, McCabe RT, Clark JT, Tuitupou A, Elgandy H, Friend DR, Kiser PF. A hot-melt extruded intravaginal ring for the sustained delivery of the antiretroviral microbicide UC781. *J Pharm Sci.* 2011
28. Gupta KM, Pearce SM, Poursaid AE, Aliyar HA, Tresco PA, Mitchnik MA, Kiser PF. Polyurethane intravaginal ring for controlled delivery of dapivirine, a nonnucleoside reverse transcriptase inhibitor of HIV-1. *J Pharm Sci.* 2008; 97(10):4228–4239. [PubMed: 18338805]
29. Kaur M, Gupta KM, Poursaid AE, Karra P, Mahalingam A, Aliyar HA, Kiser PF. Engineering a degradable polyurethane intravaginal ring for sustained delivery of dapivirine. *Drug Delivery and Translational Research.* 2011; 1(3):223–237. [PubMed: 25788241]
30. Bruce CD, Fegely KA, Rajabi-Siahboomi AR, McGinity JW. The influence of heterogeneous nucleation on the surface crystallization of guaifenesin from melt extrudates containing Eudragit L10055 or Acryl-EZE. *Eur J Pharm Biopharm.* 2010; 75(1):71–78. [PubMed: 19995604]
31. Vergnaud, J. *Controlled drug release of oral dosage forms.* Boca Raton: CRC Press; 1993.
32. Clark JT, Clark MR, Shelke NB, Johnson TJ, Smith EM, Andreasen AK, Nebeker JS, Fabian J, Friend DR, Kiser PF. Engineering a Segmented Dual-Reservoir Polyurethane Intravaginal Ring for Simultaneous Prevention of HIV Transmission and Unwanted Pregnancy. *Plos One.* 2014; 9(3)
33. Roseman TJ. Release of steroids from a silicone polymer. *J Pharm Sci.* 1972; 61(1):46–50. [PubMed: 5058644]
34. Clark JT, Johnson TJ, Clark MR, Nebeker JS, Fabian J, Tuitupou AL, Ponnappalli S, Smith EM, Friend DR, Kiser PF. Quantitative evaluation of a hydrophilic matrix intravaginal ring for the sustained delivery of tenofovir. *Journal of controlled release : official journal of the Controlled Release Society.* 2012; 163(2):240–248. [PubMed: 22981701]
35. Buckheit RW Jr, Kinjerski TL, Fliakas-Boltz V, Russell JD, Stup TL, Pallansch LA, Brouwer WG, Dao DC, Harrison WA, Schultz RJ, et al. Structure-activity and cross-resistance evaluations of a series of human immunodeficiency virus type-1-specific compounds related to oxathiin carboxanilide. *Antimicrob Agents Chemother.* 1995; 39(12):2718–2727. [PubMed: 8593008]
36. Prichard MN, Shipman C Jr. A three-dimensional model to analyze drug-drug interactions. *Antiviral Res.* 1990; 14(4–5):181–205. [PubMed: 2088205]
37. van Laarhoven JAH, Kruff MAB, Vromans H. In vitro release properties of etonogestrel and ethinyl estradiol from a contraceptive vaginal ring. *Int J Pharm.* 2002; 232(1–2):163–173. [PubMed: 11790500]
38. Lamba, N.; Woodhouse, K.; Cooper, S. *Polyurethanes in Biomedical Applications; Chapter 4: Bulk characterization and structure-property relationships of polyurethanes.* CRC Press; 1998.
39. Giron D, Goldbronn C. Place of DSC purity analysis in pharmaceutical development. *Journal of Thermal Analysis.* 1995; 44(1):217–251.
40. Chiu MH, Prenner EJ. Differential scanning calorimetry: an invaluable tool for a detailed thermodynamic characterization of macromolecules and their interactions. *Journal of Pharmacy and BioAllied Sciences.* 2011; 3(1):39–59. [PubMed: 21430954]
41. Kaur, M. Department of Bioengineering. Salt Lake City: University of Utah; 2009. Delivery of entry inhibitors using intravaginal rings for preventing the sexual transmission of HIV.
42. Higuchi T. Mechanism of Sustained-Action Medication. Theoretical Analysis of Rate of Release of Solid Drugs Dispersed in Solid Matrices. *J Pharm Sci.* 1963; 52:1145–1149. [PubMed: 14088963]
43. Chokshi RJ, Sandhu HK, Iyer RM, Shah NH, Malick AW, Zia H. Characterization of physico-mechanical properties of indomethacin and polymers to assess their suitability for hot-melt extrusion processes as a means to manufacture solid dispersion/solution. *J Pharm Sci.* 2005; 94(11): 2463–2474. [PubMed: 16200544]

44. Novak A, de la Loge C, Abetz L, van der Meulen EA. The combined contraceptive vaginal ring, NuvaRing: an international study of user acceptability. *Contraception*. 2003; 67(3):187–194. [PubMed: 12618252]
45. Van Damme L, Chandeying V, Ramjee G, Rees H, Sirivongrangson P, Laga M, Perriens J, Van Dyck E, Yai H, Karim SSA, Morar N, Dickson K, Pettifor A, Ndaba P, Richards C, Niruthisard S. Safety of multiple daily applications of COL-1492, a nonoxynol-9 vaginal gel, among female sex workers. *AIDS (London)*. 2000; 14(1):85–88.
46. Van Damme L, Govinden R, Mirembe FM, Guedou F, Solomon S, Becker ML, Pradeep BS, Krishnan AK, Alary M, Pande B, Ramjee G, Deese J, Crucitti T, Taylor D. Lack of effectiveness of cellulose sulfate gel for the prevention of vaginal HIV transmission. *N Engl J Med*. 2008; 359(5):463–472. [PubMed: 18669425]
47. Hillier SL, Moench T, Shattock R, Black R, Reichelderfer P, Veronese F. In vitro and in vivo: the story of nonoxynol 9. *J Acquir Immune Defic Syndr*. 2005; 39(1):1–8. [PubMed: 15851907]
48. Beer BE, Doncel GF, Krebs FC, Shattock RJ, Fletcher PS, Buckheit RW Jr, Watson K, Dezzutti CS, Cummins JE, Bromley E, Richardson-Harman N, Pallansch LA, Lackman-Smith C, Osterling C, Mankowski M, Miller SR, Catalone BJ, Welsh PA, Howett MK, Wigdahl B, Turpin JA, Reichelderfer P. In vitro preclinical testing of nonoxynol-9 as potential anti-human immunodeficiency virus microbicide: a retrospective analysis of results from five laboratories. *Antimicrob Agents Chemother*. 2006; 50(2):713–723. [PubMed: 16436731]
49. Ayehunie S, Cannon C, Lamore S, Kubilus J, Anderson DJ, Pudney J, Klausner M. Organotypic human vaginal-ectocervical tissue model for irritation studies of spermicides, microbicides, and feminine-care products. *Toxicol In Vitro*. 2006; 20(5):689–698. [PubMed: 16309879]
50. Smith JM, Rastogi R, Teller RS, Srinivasan P, Mesquita PM, Nagaraja U, McNicholl JM, Hendry RM, Dinh CT, Martin A, Herold BC, Kiser PF. Intravaginal ring eluting tenofovir disoproxil fumarate completely protects macaques from multiple vaginal simian-HIV challenges. *Proceedings of the National Academy of Sciences of the United States of America*. 2013; 110(40):16145–16150. [PubMed: 24043812]
51. Dobard C, Sharma S, Martin A, Pau CP, Holder A, Kuklennyk Z, Lipscomb J, Hanson DL, Smith J, Novembre FJ, Garcia-Lerma JG, Heneine W. Durable protection from vaginal simian-human immunodeficiency virus infection in macaques by tenofovir gel and its relationship to drug levels in tissue. *J Virol*. 2012; 86(2):718–725. [PubMed: 22072766]
52. Walensky RP, Park JE, Wood R, Freedberg KA, Scott CA, Bekker LG, Losina E, Mayer KH, Seage GR 3rd, Paltiel AD. The Cost-effectiveness of Pre-Exposure Prophylaxis for HIV Infection in South African Women. *Clin Infect Dis*. 2012; 54(10):1504–1513. [PubMed: 22474224]

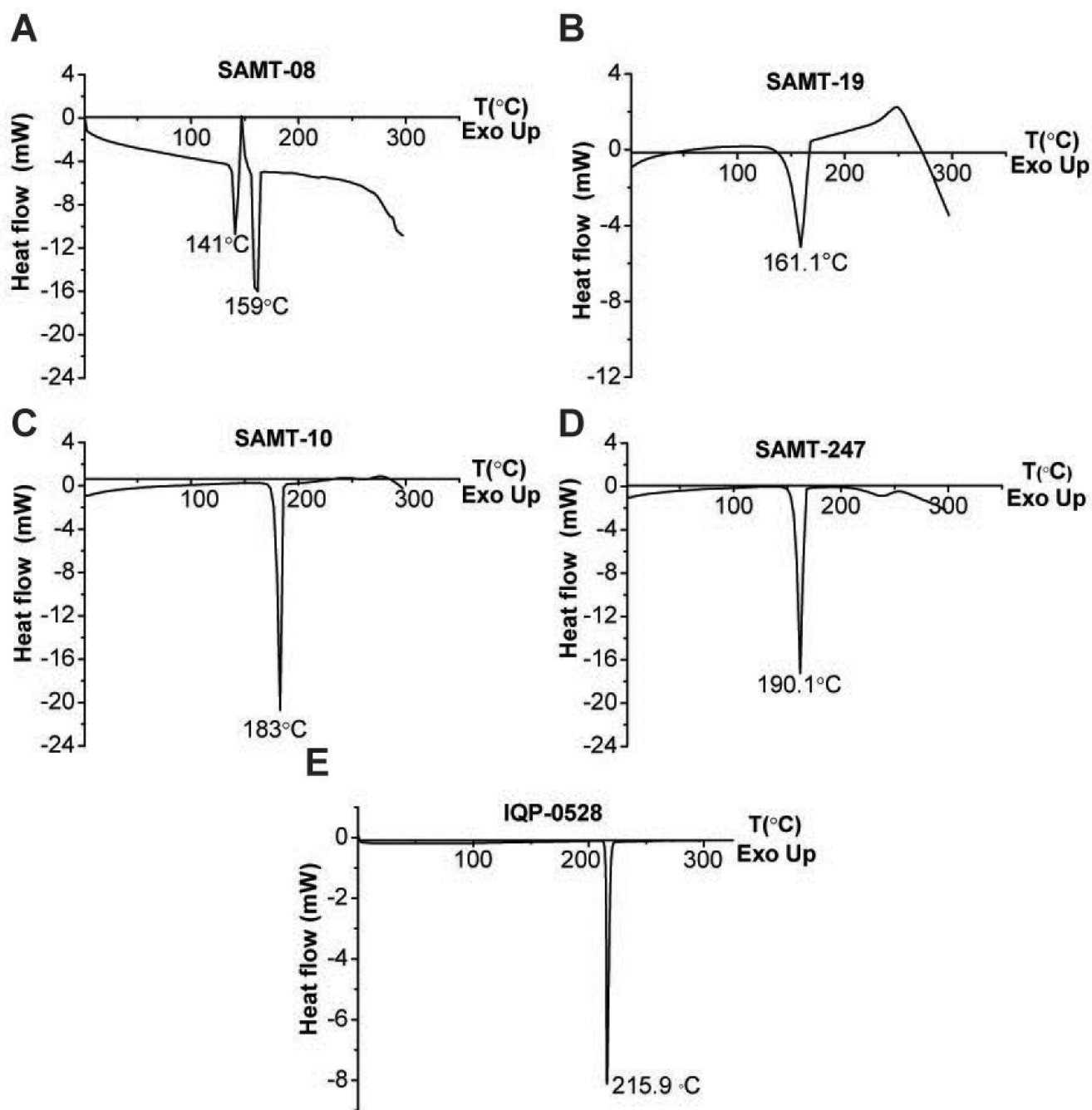


Figure 1. DSC scans of (A) SAMT-08, (B) SAMT-19, (C) SAMT-10, (D) SAMT-247 and (E) IQP-0528. The samples were heated from 0°C to 300°C at the rate of 10°C/min.

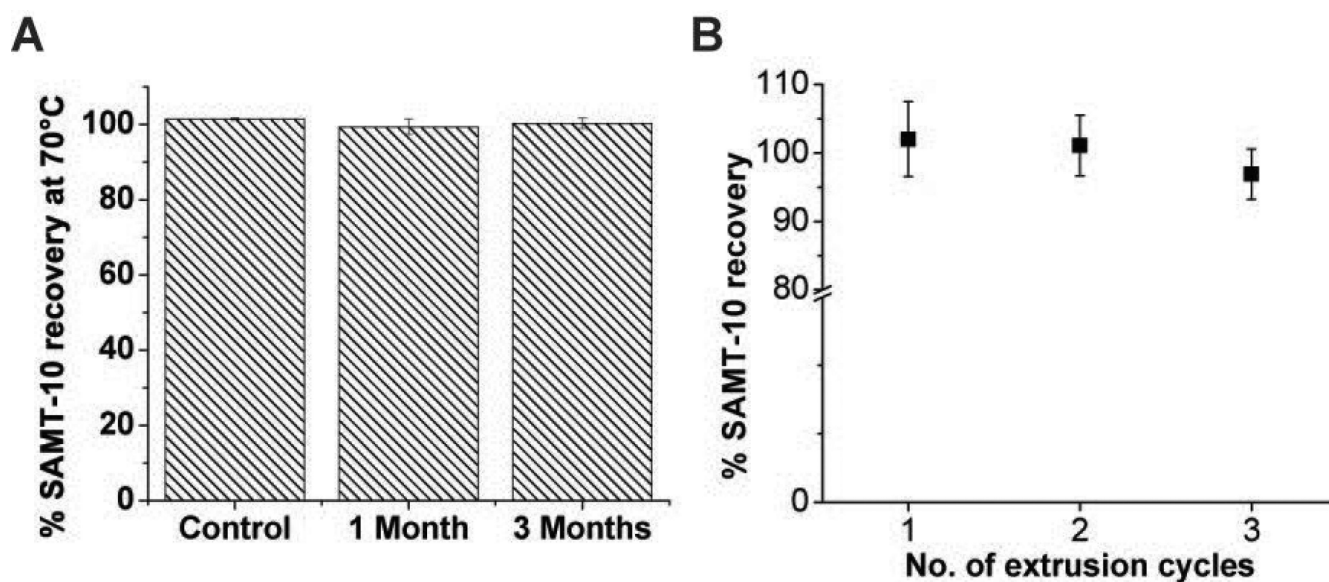


Figure 2.

(A) Dry-state stability testing of SAMT-10 at 70°C under a dry atmosphere for three months (N=3, mean \pm SD). The percent recovery of the samples at 1 and 3 months was comparable to the control sample, which was stored at -20°C throughout the study period ($p > 0.05$, Student's two-tailed *t*-test). (B) The percent recovery of SAMT-10 from the hydrophobic PEU when subjected to multiple extrusion cycles. There was no statistical significance observed in the percent recoveries between the three extrusion cycles ($p = 0.28$, one-way ANOVA).

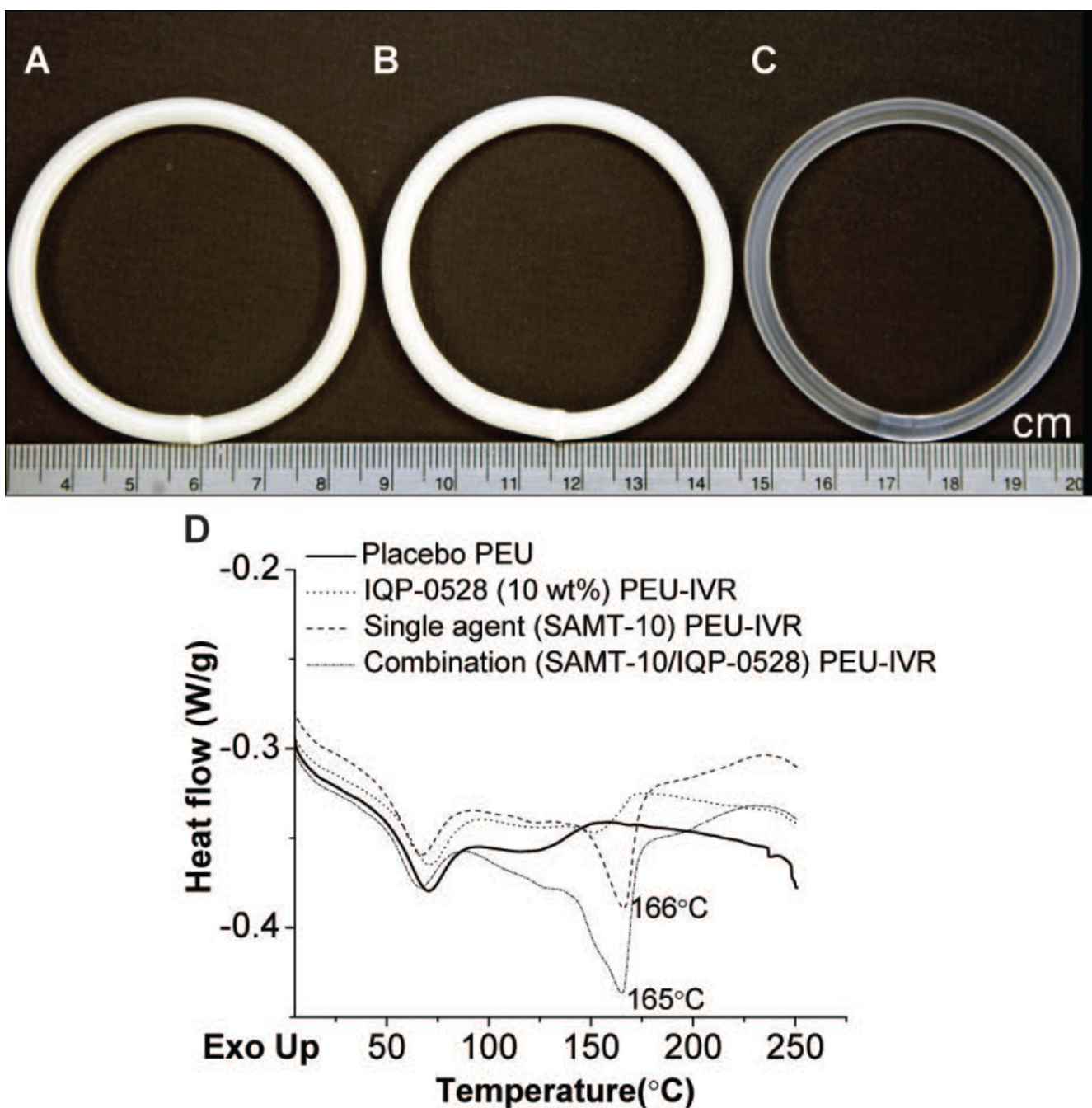


Figure 3. (A) Fabricated SAMT-10 IVR (8 wt%), (B) SAMT-10/IQP-0528 IVR (8 wt%/9 wt% respectively), and (C) the commercially available NuvaRing®. (D) DSC scans of placebo PEU, SAMT-10 (8 wt%) single agent in the PEU IVR matrix, IQP-0528 (11 wt%) single agent in the PEU IVR matrix and the combination (8 wt% SAMT-10/9 wt% IQP-0528) in the PEU IVR matrix.

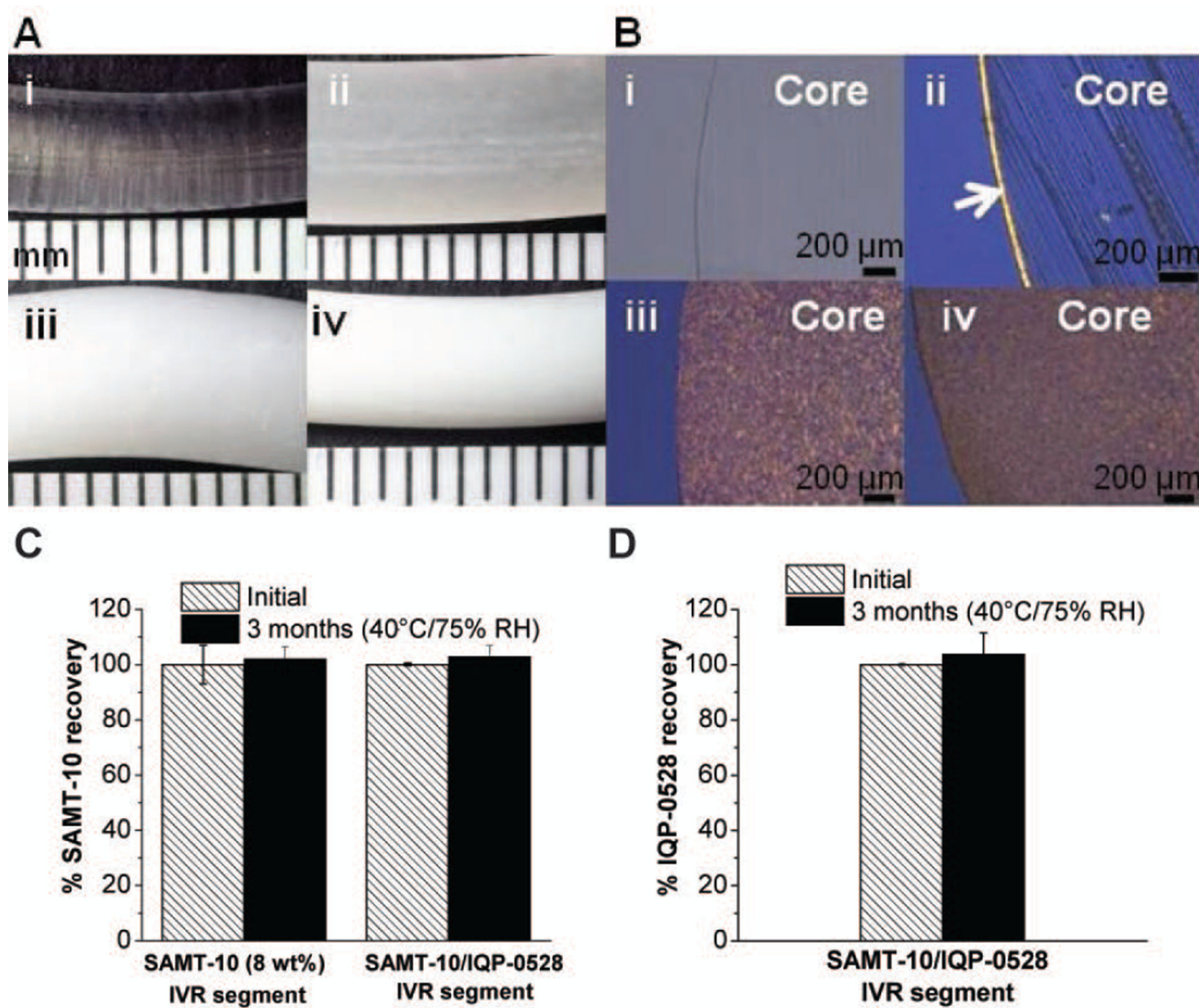


Figure 4.

Physicochemical stability of the ARV loaded IVR segments (A) Macroscopic images (under dissection scope) of placebo IVR rod segments and ARV loaded IVR segments upon 3 months storage at 50°C (i) Placebo PEU, Tecoflex EG-85A (ii) 1wt% SAMT-10 (iii) 8 wt% SAMT-10 (iv) 8 wt% SAMT-10/9 wt% IQP-0528 IVR (each mark on the scale corresponds to 1 mm). (B) Corresponding cryosectioned polarized images of the 15µm thick slice of the samples shown in Panel A. The arrow in Figure 4Bii is to indicate the surface crystallization. The scale bar on the bottom right corner is 200 µm. (C) The percent recovery of SAMT-10 from the single-agent SAMT-10 IVR (8 wt%) and the SAMT-10 (8wt%) /IQP-0528 (9 wt%) combination IVR matrix after three months of accelerated stability testing (40°C/75% RH). (D) The percent recovery of IQP-0528 from the SAMT-10 (8 wt%) /IQP-0528 (9 wt%) combination IVR matrix. The percent recoveries of the APIs at the zero time point and at three months were comparable [$p > 0.05$, Student's two-tailed t test, (N=3, mean \pm SD)].

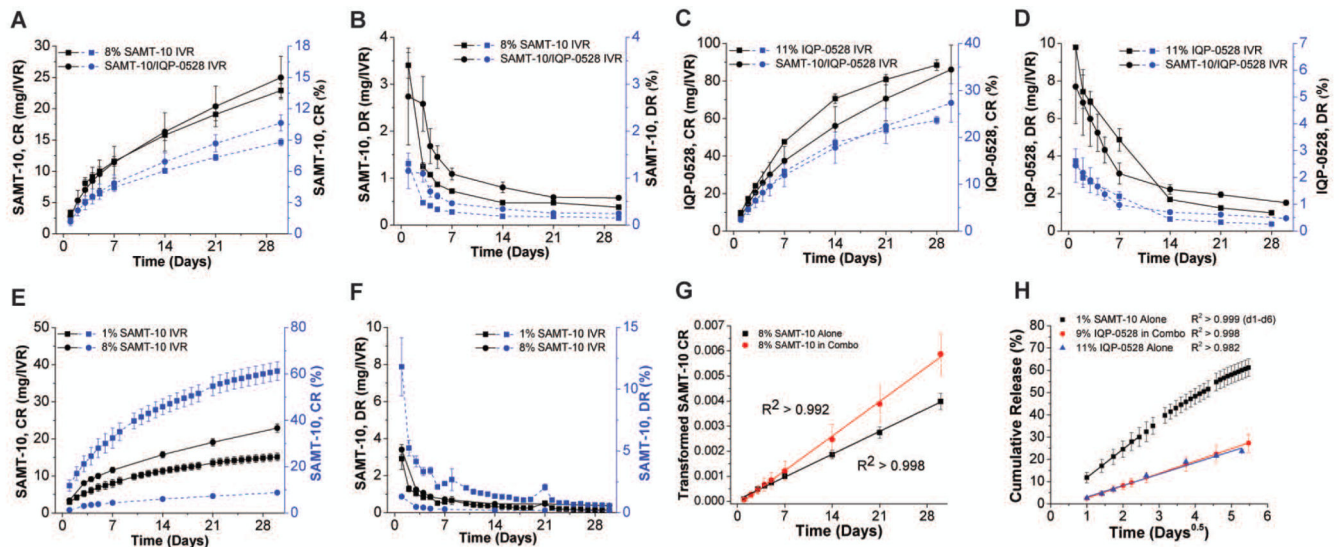


Figure 5.

(A) Cumulative release and (B) daily release rate profiles of SAMT-10, and (C) cumulative release and (D) daily release rate profiles of IQP-0528 in 25 mM acetate buffer (pH 4.2) containing Solutol[®] HS 15 (sink conditions) (N=3, mean \pm SD). Comparison of (E) cumulative release and (F) daily release between 1% and 8% SAMT-10 single agent IVR. (G) Example linear regression of transformed cumulative release against time in order to determine scaled SAMT-10 diffusivities as described in Eqn. 3. (H) Example linear regression of cumulative release against the square-root-of-time to determine ARV diffusivities as described in Eqn. 2. In G and H, a linear regression of the mean data is shown as an example, where in reality fitting was performed on individual sample curves. Coefficients of determination (R^2) were greater the value shown for all sample curves from the given IVR group.

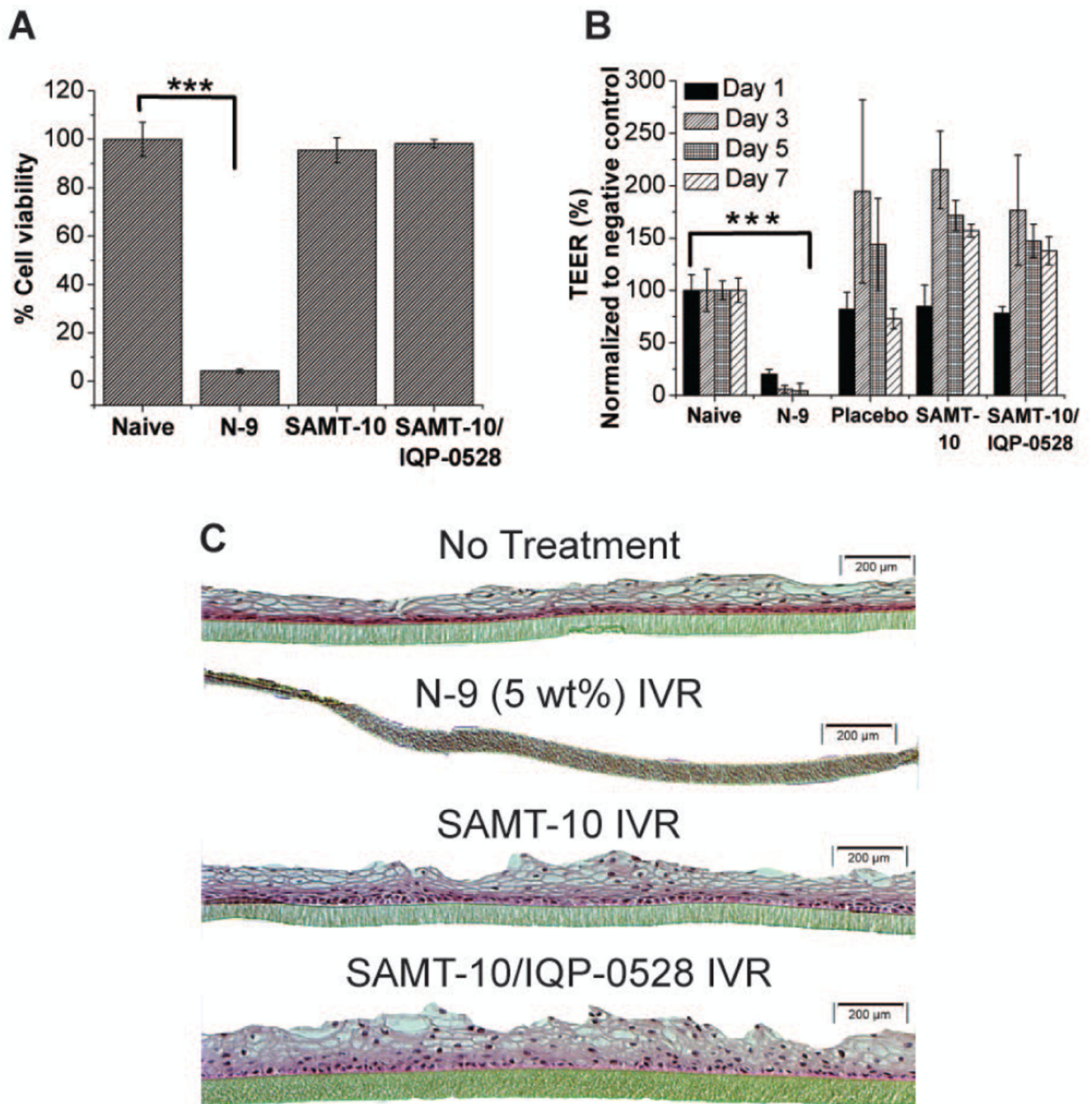


Figure 6. (A) VEC-100 tissue viability in the MTT assay after seven days of treatment with the SAMT-10 IVR (8 wt%) and the SAMT-10/IQP-0528 combination IVR. The percent viability response was compared with the naïve samples (no treatment tissues). There was no statistically significant difference between the tested IVRs and the naïve tissues, but the N-9-treated tissues showed significantly lower viability (*statistical significance, $p < 0.05$, two-tailed, Student's t test). (B) Percent TEER on days 1, 3, 5 and 7 for the control (naïve), the N-9 treated IVR segment, the placebo IVR segment and the drug-loaded IVRs. The percent

TEER for the N-9 treated tissues was significantly lower than that of the naïve tissues on all of the test days, but no significant loss in TEER was observed for the ARV-loaded formulations. (C) H&E stained images of naïve tissue, N-9-dosed tissue, SAMT-10 IVR treated tissue and SAMT-10/IQP-0528 IVR treated tissue after seven days of exposure (10X magnification). There was a complete loss of the epithelium in the N-9 dosed tissues, which indicated toxicity, whereas no epithelial erosion was observed in the drug-loaded IVR tissues.

Author Manuscript

Author Manuscript

Author Manuscript

Author Manuscript

Table 1

Structures and molecular weights (MW) of SAMT analogues and IQP-0528

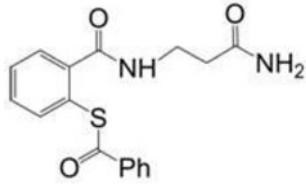
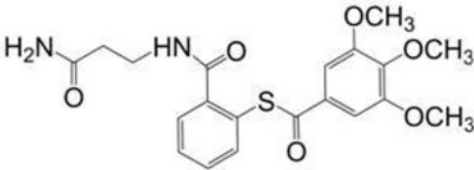
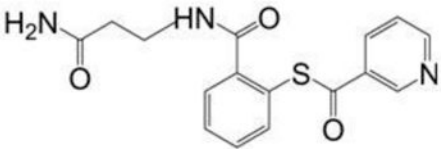
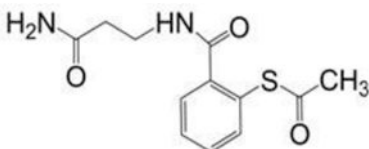
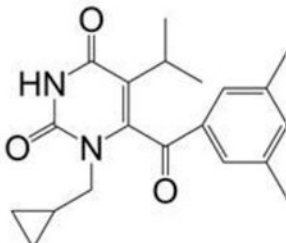
Compound	MW (g/mol)	Structure
SAMT-08	328.4	
SAMT-10	418.7	
SAMT-19	329.4	
SAMT-247	266.3	
IQP-0528	340.4	

Table 2

A: Stability of SAMT analogues in aqueous solution at pH 4.0. Data represent N=3 (mean \pm SD) or N=2 (mean). (ND – Not Detected)				
Time (weeks)	SAMT-08 (pmol/ μ L)	SAMT-10 (pmol/ μ L)	SAMT-19 (pmol/ μ L)	SAMT-247 (pmol/ μ L)
0	46.5 \pm 0.1	53.6	79.4	82
1	40.9 \pm 0.1	40.4 \pm 1	5.6	40.3 \pm 1.5
2	35.1 \pm 0.5	32.1 \pm 0.5	0.7	23.5 \pm 2
4	26.8 \pm 0.2	20.5 \pm 0.7	ND	8.0 \pm 0.6
Degradation rate constant (k) (10^{-7} sec $^{-1}$)	2.3	5.0	46.1	9.2

B: Stability of SAMT analogues in aqueous solution at pH 5.0. Data represent N=3 (mean \pm SD) or N=2 (mean). (ND – Not Detected)				
Time (weeks)	SAMT-08 (pmol/ μ L)	SAMT-10 (pmol/ μ L)	SAMT-19 (pmol/ μ L)	SAMT-247 (pmol/ μ L)
0	68.6 \pm 0.2	53	82.5	79
1	57.3 \pm 0.6	37.5	6.1 \pm 0.03	36 \pm 2.2
2	49.0 \pm 1.8	28.1	0.7 \pm 0.16	18.4 \pm 0.8
4	36 \pm 1.43	15.8	ND	6.2 \pm 0.5
Degradation rate constant (k) (10^{-7} sec $^{-1}$)	2.3	5.0	46.06	11.51

Table 3

In Vitro Efficacy of IQP-0528 and SAMT-10 Against HIV-1.

Compound	CEM-SS/HIV-1 _{IIIB}		PBMCs/HIV-1 _{ZA97/009}		HIV-1 _{RF} Cell to Cell Transmission	
	EC ₅₀ (μM)	EC ₉₅ (μM)	EC ₅₀ (μM)	EC ₉₅ (μM)	EC ₅₀ (μM)	EC ₉₅ (μM)
IQP-0528	0.002	0.008	0.006	0.019	0.006	0.085
SAMT-10	0.73	2.9	8.2	>9.6	0.53	9.1

Efficacy of IQP-0528 and SAMT-10 in standard HIV-1 cell based efficacy assays. Calculated EC₅₀ and EC₉₅ values are the average of two or three independent experiments. Within each experiment each compound concentration was evaluated in triplicate.

Table 4

Combination Antiviral Activity of IQP-0528 and SAMT-10 Tested Against HIV-1.

Assay	Synergy/Antagonism at the 95% Confidence Interval ($\mu\text{M}^2\%$)		Interpretation
	Replicate 1	Replicate 2	
CEM-SS/HIV-1 _{IIIB} CPE	162.62/-17.14	372.47/-2.36	Synergistic
PBMC/HIV-1 _{ZA/97/009} (Clade C R5)	0.22/-44.6	4.41/-25.51	Additive

Activity of the combination of IQP-0528 and SAMT-10 was evaluated against HIV-1 in CEM-SS cells and human PBMCs. These assays included two replicate antiviral combination assays. Within each replicate each compound concentration was evaluated in triplicate.

Author Manuscript

Author Manuscript

Author Manuscript

Author Manuscript